Available online at www.sciencedirect.com
ScienceDirect
Journal of Sound and Vibration 302 (2007) 789–805
JOURNAL OF SOUND AND VIBRATION
www.elsevier.com/locate/jsvi

Equilibrium and modal analyses of rotating multibeam structures employing multiple reference frames

Hong Hee Yoo[a,*], Jung Min Kim[b], Jintai Chung[c]

[a]School of Mechanical Engineering, Hanyang University, 17 Haengdang-Dong Sungdong-Gu, Seoul 133-791, Republic of Korea
[b]Daewoo Shipbuilding & Marine Engineering Co., Ltd., Jeongwang-Dong Siheung-Si, Kyonggi-Do 429-793, Republic of Korea
[c]Department of Mechanical Engineering, Hanyang University, 1271 Sa-1-Dong, Ansan, Kyunggi-Do, 425-791, Republic of Korea

Received 17 March 2006; received in revised form 27 September 2006; accepted 6 December 2006
Available online 16 February 2007

Abstract

A single reference frame is frequently employed to derive equations of motion in structural dynamic analysis. For simple structures like a single beam and a single plate, the method of employing a single reference frame usually provides well converged and accurate results for equilibrium and modal analyses. However, for structures having more general configurations such as multibeam structures, use of a single reference frame often results in slow convergence and even erroneous analysis results. In the present study, a modeling method employing multiple reference frames for dynamic equilibrium and modal analyses of rotating structures is presented. The superiority of the proposed modeling method over the single reference frame modeling method is verified with numerical examples.

1. Introduction

For the design of structures which are undergoing large overall motion during their normal operation (such as substructures of aircraft, spacecraft and ships), accurate and reliable structural modeling methods need to be employed. Even if such design activities can be most effectively supplemented by experiments, it is often very difficult and expensive to realize the actual operation environment on Earth. For instance, the gravitational field in space is much different from that on Earth. Also, fast rotational rigid-body motion, that is one of normal operation of aircraft or spacecraft substructures, is quite difficult to realize through an experiment. Therefore, designers naturally rely on analytical or numerical methods instead of experimental methods. The analytical (or numerical) methods, however, should be accurate and reliable enough for the design tasks to be accomplished with reasonable accuracy.

Several modeling methods have been developed for the dynamic analysis of structure. Classical linear modeling has been most widely used to predict the dynamic characteristics of structure (for instance, see Refs. [1–3]). This modeling method has several merits such as simplicity of formulation, ease of implementation in finite element methods, and availability of coordinate reduction techniques, which is often critically important

*Corresponding author. Tel.: +82 2 2220 0446; fax: +82 2 2293 5070.
E-mail addresses: hhyoo@hanyang.ac.kr (H.H. Yoo), jmin209@dsme.co.kr (J.M. Kim), jchung@hanyang.ac.kr (J. Chung).

0022-460X/$ - see front matter © 2007 Elsevier Ltd. All rights reserved.
doi:10.1016/j.jsv.2006.12.015

Nomenclature

$\mathbf{A}^i$	orientation matrix of the local reference frame
$\mathbf{A}^i_\theta$	partial derivative of $\mathbf{A}^i$ with respect to θ^i
$\mathbf{B}$	velocity transformation matrix
$\mathbf{C}^*$	damping matrix for independent coordinates
$\mathbf{C}^{ik}$	transformation matrix of the kth beam element in structure i
$\mathbf{I}$	3×3 identity matrix
i	structure number
j	node number
$\mathbf{K}$	total system stiffness matrix
$\mathbf{K}^*$	stiffness matrix for independent coordinates
$\mathbf{K}^i_g$	geometric stiffness matrix for structure i
k	element number
$\mathbf{L}^{ik}$	Boolean matrix of the kth beam element in structure i
l^{ik}	the length of the kth beam element in structure i
$\mathbf{M}$	total system mass matrix
$\mathbf{M}^*$	mass matrix for independent coordinates
m^{ij}	number of lumped mass of node j in structure i
$\mathbf{N}^i$	reduced modal matrix
$\mathbf{N}^{ij}$	submatrix of $\mathbf{N}^i$ related to j
$n_n{}^i$	number of nodes in structure i
O	origin of the global reference frame
$\bar{O}^i$	origin of the local reference frame
P	axial force
P^{ik}	axial force acting on the beam element k in structure i
$\mathbf{Q}$	total generalized force
$\mathbf{Q}_g$	generalized force due to geometric stiffening effect
$\mathbf{Q}^i_g$	generalized force due to geometric stiffening effect for structure i
$\mathbf{Q}_v$	generalized force due to centrifugal and Coriolis accelerations
$\mathbf{q}$	total system coordinates of the system
$\mathbf{q}_d$	dependent coordinates
$\mathbf{q}_i$	independent coordinates
$\mathbf{q}^i$	coordinates for structure i
$\mathbf{q}^i_f$	modal coordinates for the structure i
$\mathbf{R}^i$	position of the origin point of structure i
$\mathbf{r}^{ij}$	position of the generic node j
$\mathbf{S}^{ik}$	shape function of the beam element k in structure i
$\mathbf{S}^{ik}_{2,x}$	partial derivative of $\mathbf{S}^{ij}_2$ with respect to x
s	stretching variable
T^i	kinetic energy of structure i
u_2	bending displacement
u^{ik}_2	bending displacement of the beam element k in structure i
U^i	strain energy of structure i
$\bar{\mathbf{u}}^{ij}$	deformed position of node j in structure i
$\bar{\mathbf{u}}^i_f$	elastic deformation of the generic structure i
$\bar{\mathbf{u}}^{ij}_f$	elastic deformation of node j in structure i
$\bar{\mathbf{u}}^{ij}_r$	undeformed position of node j in structure i
$\delta W_g{}^i$	virtual work done by the axial force to the structure i
$W_g{}^{ik}$	work done by the axial force P^{ik} to the element k in structure i
$X-Y$	global reference frame
$\bar{X}^i - \bar{Y}^i$	local reference frame
$\bar{x}^{ik} - \bar{y}^{ik}$	element reference frame
α^{ik}	angle between local reference frame $\bar{X}^i - \bar{Y}^i$ and element reference frame $\bar{x}^{ik} - \bar{y}^{ik}$
β	angle between two beam elements
$\boldsymbol{\lambda}$	Lagrange multiplier
$\boldsymbol{\Phi}$	algebraic constraint equation
$\boldsymbol{\Phi}_\mathbf{q}$	Jacobian matrix (partial derivative of $\boldsymbol{\Phi}$ with respect to $\mathbf{q}$)
$\boldsymbol{\Phi}_{\mathbf{q}d}$	partial derivative of $\boldsymbol{\Phi}$ with respect to $\mathbf{q}_d$
$\boldsymbol{\Phi}_{\mathbf{q}i}$	partial derivative of $\boldsymbol{\Phi}$ with respect to $\mathbf{q}_i$
θ^i	rotational coordinates for the structure i
Ω_s	steady-state angular velocity

for the dynamic analysis of structures. However, the classical modeling method often displays a critical flaw when the structure undergoes a large overall motion. Consequently, several nonlinear modeling methods (for instance, see Refs. [4,5]) were developed to resolve the problem of the classical modeling method. However, these methods are inconvenient (so inefficient) for the modal analysis of structures undergoing overall motion. A three-step procedure (first finding the dynamic equilibrium state, then linearizing the nonlinear equations at

the equilibrium state, and finally performing modal analysis with the linearized equations) needs to be employed to obtain the modal characteristics of rotating structures. More recently, to avoid the inconvenience of the nonlinear modeling methods, special linear modeling methods employing hybrid deformation variables (for instance, see Refs. [6–9]) were introduced. However, only simple structures (a single beam and a single plate) were solved with the modeling methods, in which a single reference frame is employed. This method of employing single reference frame is also applied to analyze composite structures (for instance, see Refs. [10–13]) successfully.

For the modeling methods mentioned so far, a single reference frame (an inertial reference frame is employed for the nonlinear modeling methods and a local reference frame is employed for the special linear modeling methods) is employed. The method of employing a single reference frame is simple and effective to analyze structures like a single beam and a single plate (see Refs. [4,14]). However, for structures having more general configurations, slow convergence and even erroneous results could be often experienced with the method. Therefore, a modeling method which can provide well converged and accurate results needs to be developed for structures having more general and complex configurations.

In this paper, a modeling method employing multiple reference frames is proposed. Compared to the single reference frame modeling method (implemented in most commercial codes), this method provides accurate dynamic response and modal characteristics for structures having more general and complex configurations. If the structure has a simple geometry like a beam or a plate, the accuracy of the proposed method is equivalent to the method of employing single reference frame. However, if the structure has a general complex configuration, the proposed method clearly exhibits its superiority over the single reference frame method.

The proposed modeling method employs finite element method to consider structures having more general and complex configuration. The modeling method employs lumped mass modeling technique that simplifies the derivation of equations of motion. The mass and the stiffness matrices can be easily obtained from any finite element codes for static and dynamic analysis of structures. Elastic deformations are approximated with the modal matrix, which can be obtained from the mass and the stiffness matrices by solving the eigenvalue problem. Geometric stiffening effect that results from the centrifugal inertia force caused by large overall rigid-body motion is considered in the modeling method. To verify the rapid convergence and the accuracy of the proposed modeling method, some numerical examples are solved. The results obtained by the present modeling method employing multiple reference frames are compared to those obtained by the modeling method employing a single reference frame. The superiority of the present modeling method over the method employing a single reference frame is verified with the numerical examples.

2. Equations of motion

2.1. Kinetic energy

Fig. 1 shows the configuration of a generic structure i undergoing rigid-body motion and elastic deformation. The index j denotes a generic node of the generic structure. In the figure, $X-Y$ denotes a global reference frame, O denotes the origin of the global reference frame, $\bar{X}^i-\bar{Y}^i$ denotes a local reference frame, and $\bar{O}^i$ denotes the origin of the local reference frame. The column matrices $\mathbf{R}^i$ and $\mathbf{r}^{ij}$, respectively, denote the position of $\bar{O}^i$ and the generic node, which are measured in the global reference frame. The column matrices $\bar{\mathbf{u}}_r^{ij}$, $\bar{\mathbf{u}}_f^{ij}$, and $\bar{\mathbf{u}}^{ij}$, respectively denote the undeformed position of node j from $\bar{O}^i$, the elastic deformation of node j, and the deformed position of node j from $\bar{O}^i$, which are measured in the reference frame. Using the notations introduced so far, the following relation can be obtained:

$$\mathbf{r}^{ij} = \mathbf{R}^i + \mathbf{A}^i\bar{\mathbf{u}}^{ij} = \mathbf{R}^i + \mathbf{A}^i\left(\bar{\mathbf{u}}_r^{ij} + \bar{\mathbf{u}}_f^{ij}\right), \tag{1}$$

where $\mathbf{A}^i$ is the orientation matrix of the local reference frame with respect to the global reference frame.

If $\bar{\mathbf{u}}_f^i$ represents the elastic deformation of the generic structure i, it can be constituted by $\bar{\mathbf{u}}_f^{ij}$, which is defined previously. The elastic deformation $\bar{\mathbf{u}}_f^i$ can be obtained as follows:

$$\bar{\mathbf{u}}_f^i = \mathbf{N}^i\mathbf{q}_f^i, \tag{2}$$

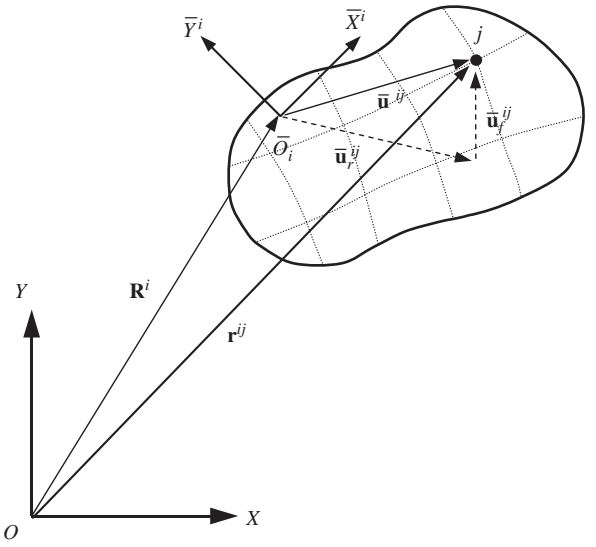

Fig. 1. Configuration of a structure undergoing rigid-body motion and elastic deformation.

where $\mathbf{N}^i$ denotes a reduced modal matrix, which can be obtained by solving the eigenvalue problem of the generic structure and $\mathbf{q}_f^i$ denotes the modal coordinate. The reduced modal matrix includes only some mode vectors (not all mode vectors). Since $\bar{\mathbf{u}}_f^{ij}$ is a sub-matrix of $\bar{\mathbf{u}}_f^i$, it can be also obtained by using the modal matrix as follows:

$$\bar{\mathbf{u}}_f^{ij} = \mathbf{N}^{ij}\mathbf{q}_f^i, \tag{3}$$

where $\mathbf{N}^{ij}$ is a sub-matrix of $\mathbf{N}^i$ related to node j.

Now the velocity of node j can be obtained by substituting Eq. (3) into Eq. (1) and differentiating the resulting equation with respect to time:

$$\dot{\mathbf{r}}^{ij} = \dot{\mathbf{R}}^i + \mathbf{B}^{ij}\dot{\theta}^i + \mathbf{A}^i\mathbf{N}^{ij}\dot{\mathbf{q}}_f^i, \tag{4}$$

where

$$\mathbf{B}^{ij} \equiv \mathbf{A}_\theta^i \bar{\mathbf{u}}^{ij} \tag{5}$$

and θ^i consists of rotational coordinates of the local reference frame with respect to the global reference frame and $\mathbf{A}_\theta{}^i$ is the partial derivative of $\mathbf{A}^i$ with respect to θ^i. Now the kinetic energy of the structure i can be described as follows:

$$T^i = \frac{1}{2}\dot{\mathbf{q}}^{i\mathrm{T}}\mathbf{M}^i\dot{\mathbf{q}}^i, \tag{6}$$

where

$$\mathbf{M}^i = \begin{bmatrix} \mathbf{M}_{rr}^i & \mathbf{M}_{r\theta}^i & \mathbf{M}_{rf}^i \\ (\mathbf{M}_{r\theta}^i)^{\mathrm{T}} & \mathbf{M}_{\theta\theta}^i & \mathbf{M}_{\theta f}^i \\ (\mathbf{M}_{rf}^i)^{\mathrm{T}} & (\mathbf{M}_{\theta f}^i)^{\mathrm{T}} & \mathbf{M}_{ff}^i \end{bmatrix}, \quad \mathbf{q}^i = \begin{Bmatrix} \mathbf{R}^i \\ \theta^i \\ \mathbf{q}_f^i \end{Bmatrix}. \tag{7}$$

The sub-matrices of $\mathbf{M}^i$ are given as follows:

$$\mathbf{M}_{rr}^i = \sum_{j=1}^{n_n^i} m^{ij}\mathbf{I}, \quad \mathbf{M}_{r\theta}^i = \sum_{j=1}^{n_n^i} m^{ij}\mathbf{B}^{ij}, \quad \mathbf{M}_{rf}^i = \sum_{j=1}^{n_n^i} m^{ij}\mathbf{A}^i\mathbf{N}^{ij}, \tag{8}$$

$$\mathbf{M}^i_{\theta\theta} = \sum_{j=1}^{n_n^i} m^{ij}\mathbf{B}^{ij^{\mathrm{T}}}\mathbf{B}^{ij}, \quad \mathbf{M}^i_{\theta f} = \sum_{j=1}^{n_n^i} m^{ij}\mathbf{B}^{ij^{\mathrm{T}}}\mathbf{A}^i\mathbf{N}^{ij}, \quad \mathbf{M}^i_{ff} = \sum_{j=1}^{n_n^i} m^{ij}\mathbf{N}^{ij^{\mathrm{T}}}\mathbf{N}^{ij}. \tag{9}$$

In Eqs. (8) and (9), m^{ij} denotes the lumped mass of node j, ${n_n}^i$ is the number of nodes in structure i, and $\mathbf{I}$ denotes 3×3 identity matrix.

2.2. Strain energy

Since the strain energy of the structure i is only associated with elastic deformation, it can be described as follows:

$$U^i = \tfrac{1}{2}\bar{\mathbf{u}}_f^{i^{\mathrm{T}}}\bar{\mathbf{K}}^i\bar{\mathbf{u}}_f^i, \tag{10}$$

where $\bar{\mathbf{K}}^i$ is the global stiffness matrix of the structure. If Eq. (2) is employed, the strain energy can be rewritten as follows:

$$U^i = \tfrac{1}{2}\mathbf{q}^{i^{\mathrm{T}}}\mathbf{K}^i\mathbf{q}^i, \tag{11}$$

where

$$\mathbf{K}^i = \mathbf{N}^{i^{\mathrm{T}}}\bar{\mathbf{K}}^i\mathbf{N}^i. \tag{12}$$

The stiffness matrix expression given in Eq. (12) is different from the mass matrix expression of Eq. (7), which is dependent on the orientation matrix. Since the strain energy has nothing to do with the rigid-body rotation of the structure, the stiffness matrix does not depend on the orientation matrix.

In the present work, Euler–Bernoulli beam theory is employed and the corresponding strain energy expression is employed for Eq. (11). So, the shear and the rotary inertia effects are not considered. Such effects should be included for the analysis if the beam has relatively thick dimension. Since the major issue of the present work does not lie on issues of elastic effects, those effects are not considered. The major contribution of the present work lies on the issue of the accuracy enhancement due to employment of multiple reference frames.

2.3. Generalized force due to geometric stiffening effect

To consider the geometric stiffening effect of a structure that consists of beam elements, work done by the axial force P during the lateral deflection should be considered. The geometric stiffening effect of an infinitesimal beam element due to lateral deflection is shown in Fig. 2. The axial length change of the infinitesimal beam element due to lateral deflection can be obtained as follows:

$$\mathrm{d}x - \mathrm{d}s = \mathrm{d}x - \left[(\mathrm{d}x)^2 - \left(\frac{\partial u_2}{\partial x}\right)^2(\mathrm{d}x)^2\right]^{1/2} \cong \frac{1}{2}\left(\frac{\partial u_2}{\partial x}\right)^2 \mathrm{d}x. \tag{13}$$

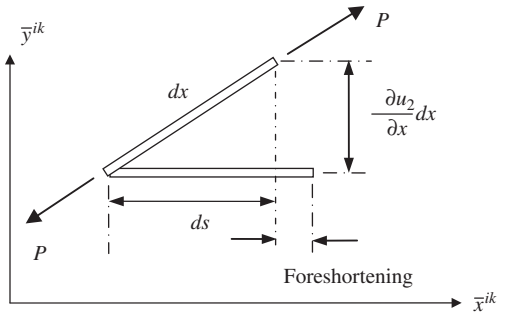

Fig. 2. Foreshortening of an infinitesimal beam element due to lateral deflection.

Since foreshortening occurs while the axial force acts on the element, the work done by the axial force is negative. Therefore, the work done by the axial force, which is invariant during the foreshortening, can be obtained as follows:

$$W_g^{ik} = -\frac{1}{2}\int_0^{l^{ik}} P^{ik}\left(\frac{\partial u_2^{ik}}{\partial x}\right)^2 \mathrm{d}x, \tag{14}$$

where l^{ik} is the length of the kth beam element in the structure i; P^{ik} is the axial force acting on the beam element; u_2^{ik} is the lateral deflection of the beam element. Therefore, the virtual work done by the axial force of the structure i that is composed of n_e^i beam elements can be described as following equation:

$$\delta W_g^i = -\sum_{k=1}^{n_e^i}\int_0^{l^{ik}} P^{ik}\left(\frac{\partial u_2^{ik}}{\partial x}\right)\delta\left(\frac{\partial u_2^{ik}}{\partial x}\right)\mathrm{d}x, \tag{15}$$

where n_e^i is the number of beam elements of the structure i.

By employing the shape function $\mathbf{S}^{ik}$ of a beam element, the axial and lateral deflection of beam element can be written as follows:

$$\begin{bmatrix} u_1^{ik} \\ u_2^{ik} \end{bmatrix} = \mathbf{S}^{ik}\mathbf{T}^{ik}\mathbf{q}_f^i. \tag{16}$$

The shape function $\mathbf{S}^{ik}$ and $\mathbf{T}^{ik}$ in Eq. (16) can be given as follows:

$$\mathbf{S}^{ik} = \begin{bmatrix} \mathbf{S}_1^{ik} \\ \mathbf{S}_2^{ik} \end{bmatrix} = \begin{bmatrix} 1-\xi & 0 & 0 & \xi & 0 & 0 \\ 0 & 1-3\xi^2+2\xi^3 & l^{ij}(\xi-2\xi^2+\xi^3) & 0 & 3\xi^2-2\xi^3 & l^{ij}(\xi^3-\xi^2) \end{bmatrix}, \tag{17}$$

where

$$\xi = \frac{x}{l^{ik}}, \tag{18}$$

$$\mathbf{T}^{ik} \equiv \mathbf{C}^{ik}\mathbf{L}^{ik}\mathbf{N}^i, \tag{19}$$

where

$$\mathbf{C}^{ij} = \begin{bmatrix} \cos\alpha^{ik} & \sin\alpha^{ik} & 0 & 0 & 0 & 0 \\ -\sin\alpha^{ik} & \cos\alpha^{ik} & 0 & 0 & 0 & 0 \\ 0 & 0 & 1 & 0 & 0 & 0 \\ 0 & 0 & 0 & \cos\alpha^{ik} & \sin\alpha^{ik} & 0 \\ 0 & 0 & 0 & -\sin\alpha^{ik} & \cos\alpha^{ik} & 0 \\ 0 & 0 & 0 & 0 & 0 & 1 \end{bmatrix}, \tag{20}$$

$$\mathbf{L}^{ik} = \begin{bmatrix} 0 & \overbrace{\ldots\ 0}^{6(m-1)} & 1 & 0 & 0 & 0 & \ldots & 0 & 0 & 0 & 0 & 0 & \ldots & 0 \\ 0 & \ldots\ 0 & 0 & 1 & 0 & 0 & \ldots & 0 & 0 & 0 & 0 & 0 & \ldots & 0 \\ 0 & \ldots\ 0 & 0 & 0 & 1 & 0 & \ldots & 0 & 0 & 0 & 0 & 0 & \ldots & 0 \\ 0 & \ldots\ 0 & 0 & 0 & 0 & 0 & \ldots & 0 & 1 & 0 & 0 & 0 & \ldots & 0 \\ 0 & \ldots\ 0 & 0 & 0 & 0 & 0 & \ldots & 0 & 0 & 1 & 0 & 0 & \ldots & 0 \\ 0 & \ldots\ \underbrace{0}_{6(n-1)} & 0 & 0 & 0 & 0 & \ldots & 0 & 0 & 0 & 1 & 0 & \ldots & 0 \end{bmatrix} \tag{21}$$

In the above equations, $\mathbf{C}^{ik}$ and $\mathbf{L}^{ik}$ denote a transformation matrix and a Boolean matrix for beam element assembly, respectively. The Boolean matrix is often employed for the connectivity of finite elements

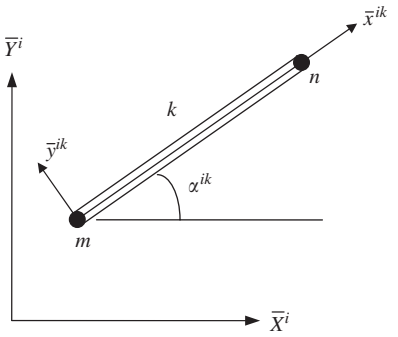

Fig. 3. Notations for kth beam element.

(see Ref. [15]). The total size of the Boolean matrix is $6 \times 3n_n^i$. In Eq. (20), α^{ik} denotes the angle between the structure reference frame $\bar{X}^i - \bar{Y}^i$ and the element reference frame $\bar{x}^{ik} - \bar{y}^{ik}$. In Eq. (21), m and n denote the node numbers of the kth beam element, which are shown in Fig. 3.

Substituting Eq. (16) into Eq. (15), the virtual work created by the geometric stiffening effect can be obtained as follows:

$$\delta W_g^i = -\mathbf{q}_f^{i\mathrm{T}} \mathbf{K}_g^{i\mathrm{T}} \delta \mathbf{q}_f^i. \tag{22}$$

In the above equation, $\mathbf{K}_g^i$ is the geometric stiffness matrix for structure i which can be defined as

$$\mathbf{K}_g^i \equiv \sum_{k=1}^{n_e^i} P^{ik} \mathbf{T}^{ik\mathrm{T}} \mathbf{G}^{ik} \mathbf{T}^{ik}, \tag{23}$$

where

$$\mathbf{G}^{ik} \equiv \int_0^{l^{ik}} \mathbf{S}_{2,x}^{ikT} \mathbf{S}_{2,x}^{ik} \, \mathrm{d}x = \frac{1}{l^{ik}} \begin{bmatrix} 0 & 0 & 0 & 0 & 0 & 0 \\ 0 & \frac{6}{5} & \frac{l^{ik}}{10} & 0 & -\frac{6}{5} & \frac{l^{ik}}{10} \\ 0 & \frac{l^{ik}}{10} & \frac{2(l^{ik})^2}{15} & 0 & -\frac{l^{ik}}{10} & -\frac{(l^{ik})^2}{30} \\ 0 & 0 & 0 & 0 & 0 & 0 \\ 0 & -\frac{6}{5} & -\frac{l^{ik}}{10} & 0 & \frac{6}{5} & -\frac{l^{ik}}{10} \\ 0 & \frac{l^{ik}}{10} & -\frac{(l^{ik})^2}{30} & 0 & -\frac{l^{ik}}{10} & \frac{2(l^{ik})^2}{15} \end{bmatrix}, \tag{24}$$

where $\mathbf{S}_{2,x}{}^{ik}$ is the partial derivative of $\mathbf{S}_2^{ik}$ with respect to x. Using the Hooke's law, the axial force P^{ik} can be obtained as follows:

$$P^{ik} = E^{ik} a^{ik} \left(\frac{\partial u_1^{ik}}{\partial x} \right) = E^{ik} a^{ik} \mathbf{S}_{1,x}^{ik} \mathbf{q}_f^i, \tag{25}$$

where E^{ik} is the Young's modulus of the beam element k in the structure i, a^{ik} is the cross sectional area of the element and

$$\mathbf{S}_{1,x}^{ik} = \frac{1}{l^{ik}} [-1 \quad 0 \quad 0 \quad 1 \quad 0 \quad 0]. \tag{26}$$

From Eq. (22), the generalized force due to geometric stiffening effect associated with $\mathbf{q}_f^i$ can be obtained as follows:

$$(\mathbf{Q}_g^i)_f = -\mathbf{K}_g^i \mathbf{q}_f^i. \tag{27}$$

Finally, the generalized force can be expressed as follows:

$$\mathbf{Q}_g^i = \begin{Bmatrix} 0 \\ 0 \\ 0 \\ (\mathbf{Q}_g^i)_f \end{Bmatrix}. \tag{28}$$

2.4. Equations of motion

Using the kinetic energy, the strain energy, and the generalized force due to geometric stiffening effect, the equations of motion of a structure that consists of *nb* substructures can be derived (see Ref. [16]) as follows:

$$\mathbf{M}\ddot{\mathbf{q}} + \mathbf{K}\mathbf{q} + \mathbf{\Phi}_q^{\mathrm{T}}\boldsymbol{\lambda} = \mathbf{Q}_v + \mathbf{Q}_g. \tag{29}$$

In the above equation, $\mathbf{M}$ and $\mathbf{K}$ are the system mass and stiffness matrices which are defined as follows:

$$\mathbf{M} = \begin{bmatrix} \mathbf{M}^1 & 0 & 0 & 0 & 0 \\ 0 & \mathbf{M}^2 & 0 & 0 & 0 \\ 0 & 0 & \cdot & 0 & 0 \\ 0 & 0 & 0 & \cdot & 0 \\ 0 & 0 & 0 & 0 & \mathbf{M}^{nb} \end{bmatrix}, \tag{30}$$

$$\mathbf{K} = \begin{bmatrix} \mathbf{K}^1 & 0 & 0 & 0 & 0 \\ 0 & \mathbf{K}^2 & 0 & 0 & 0 \\ 0 & 0 & \cdot & 0 & 0 \\ 0 & 0 & 0 & \cdot & 0 \\ 0 & 0 & 0 & 0 & \mathbf{K}^{nb} \end{bmatrix}. \tag{31}$$

And $\mathbf{q}$ consists of total generalized coordinates of the system, $\mathbf{\Phi}_\mathbf{q}$ and $\boldsymbol{\lambda}$ are the Jacobian matrix and the corresponding Lagrange multiplier which result from algebraic constraint equations. The notation $\mathbf{Q}_v$ denotes the generalized force (due to centrifugal and Coriolis acceleration components) which is given as follows:

$$\mathbf{Q}_v = \begin{Bmatrix} \mathbf{Q}_v^1 \\ \cdot \\ \cdot \\ \cdot \\ \mathbf{Q}_v^{nb} \end{Bmatrix}, \tag{32}$$

where

$$\mathbf{Q}_v^i = -\dot{\mathbf{M}}^i \dot{\mathbf{q}}^i + \frac{1}{2}\left[\frac{\partial}{\partial \mathbf{q}^i}\left(\dot{\mathbf{q}}^{i\mathrm{T}} \mathbf{M}^i \dot{\mathbf{q}}^i\right)\right]^{\mathrm{T}}. \tag{33}$$

And the generalized force of the system due to the geometric stiffening effect is given as follows:

$$\mathbf{Q}_g = \begin{Bmatrix} \mathbf{Q}_g^1 \\ \cdot \\ \cdot \\ \cdot \\ \mathbf{Q}_g^{nb} \end{Bmatrix}. \tag{34}$$

2.5. Equations for modal analysis

To perform modal analysis of rotating structures, the dynamic equilibrium position and the linearized equations of motion at the equilibrium position need to be derived (to obtain the mass and the stiffness matrices). Due to the algebraic constraint equations $\mathbf{\Phi}$ the system coordinates $\mathbf{q}$ are not independent. To obtain the dynamic equilibrium position effectively, the equations of motion, Eq. (29), need to be expressed with independent coordinates only. For the purpose, the system coordinates of $\mathbf{q}$ are partitioned as follows:

$$\mathbf{q} = \begin{Bmatrix} \mathbf{q}_d \\ \mathbf{q}_i \end{Bmatrix}, \tag{35}$$

where $\mathbf{q}_d$ and $\mathbf{q}_i$ represent the dependent and the independent coordinates, respectively. To describe the configuration of a multibody system, 6 Cartesian coordinates (3 for position and 3 for orientation) are often employed for the general formulation of multibody dynamics. Since the number of degrees of freedom is far less than the number of Cartesian coordinates, one may choose only some coordinates as the independent coordinates. The method of choosing independent coordinates can be found in previous literature (see Ref. [16]).

To find the velocity transformation relation between system coordinates and the independent coordinates, the algebraic constraint equations $\mathbf{\Phi}$ are differentiated with respect to time:

$$\mathbf{\Phi}_{\mathbf{q}_d}\dot{\mathbf{q}}_d + \mathbf{\Phi}_{\mathbf{q}_i}\dot{\mathbf{q}}_i + \mathbf{\Phi}_t = 0. \tag{36}$$

In this study, it is assumed that the algebraic constraint equations are not explicit functions of time. So,

$$\dot{\mathbf{q}}_d = -\mathbf{\Phi}_{\mathbf{q}_d}^{-1}\mathbf{\Phi}_{\mathbf{q}_i}\dot{\mathbf{q}}_i, \tag{37}$$

Thus, the system coordinates can be expressed as follows:

$$\dot{\mathbf{q}} = \mathbf{B}\dot{\mathbf{q}}_i, \tag{38}$$

where

$$\mathbf{B} = \begin{bmatrix} -\mathbf{\Phi}_{\mathbf{q}_d}^{-1}\mathbf{\Phi}_{\mathbf{q}_i} \\ \mathbf{I} \end{bmatrix}. \tag{39}$$

The matrix $\mathbf{B}$ is often called the velocity transformation matrix. Differentiating Eq. (38) with respect to time,

$$\ddot{\mathbf{q}} = \mathbf{B}\ddot{\mathbf{q}}_i + \boldsymbol{\gamma}, \tag{40}$$

where

$$\boldsymbol{\gamma} = \dot{\mathbf{B}}\dot{\mathbf{q}}_i. \tag{41}$$

Now substituting Eq. (40) into Eq. (29) and pre-multiplying the resulting equation by $\mathbf{B}^{\mathrm{T}}$, one can obtain the following equation (since $\mathbf{B}$ is the null space of $\mathbf{\Phi}_{\mathbf{q}}$):

$$\mathbf{B}^{\mathrm{T}}\mathbf{M}\mathbf{B}\ddot{\mathbf{q}}_i + \mathbf{B}^{\mathrm{T}}(\mathbf{M}\boldsymbol{\gamma} - \mathbf{Q}) = 0, \tag{42}$$

where

$$\mathbf{Q} = -\mathbf{K}\mathbf{q} + \mathbf{Q}_v + \mathbf{Q}_g. \tag{43}$$

From Eq. (42), one can obtain the dynamic equilibrium position by letting $\dot{\mathbf{q}}_i = \ddot{\mathbf{q}}_i = 0$. Thus,

$$\mathbf{B}^{\mathrm{T}}\mathbf{Q} = 0. \tag{44}$$

Since the above equation is generally nonlinear in terms of the independent coordinates, the dynamic equilibrium position can be obtained by using Newton–Raphson algorithm. Finally, the modal equations can be obtained by linearizing equation (42) at the dynamic equilibrium position. Thus, the mass, the damping, and the stiffness matrices for the modal analysis are obtained as follows:

$$\mathbf{M}^* = \mathbf{B}^{\mathrm{T}}\mathbf{M}\mathbf{B}\big|_{\mathbf{q}_i=\mathbf{q}_i^*}, \tag{45}$$

$$\mathbf{C}^* = \left[\frac{\partial}{\partial \dot{\mathbf{q}}_i}\left(\mathbf{B}^{\mathrm{T}}\mathbf{M}\mathbf{B}\ddot{\mathbf{q}}_i + \mathbf{B}^{\mathrm{T}}(\mathbf{M}\boldsymbol{\gamma} - \mathbf{Q})\right)\right]_{\mathbf{q}_i=\mathbf{q}_i^*}, \tag{46}$$

$$\mathbf{K}^* = \left[\frac{\partial}{\partial \mathbf{q}_i}\left(\mathbf{B}^{\mathrm{T}}\mathbf{M}\mathbf{B}\ddot{\mathbf{q}}_i + \mathbf{B}^{\mathrm{T}}(\mathbf{M}\boldsymbol{\gamma} - \mathbf{Q})\right)\right]_{\mathbf{q}_i=\mathbf{q}_i^*}, \tag{47}$$

where $\mathbf{q}_i^*$ is the independent coordinates at the dynamic equilibrium position. To obtain the damping and stiffness matrices, the finite difference method is employed in the present study. Obtaining the damping and the stiffness matrices in an analytical way is too complicated and time consuming. Furthermore, the finite difference method could provide good accuracy as well as efficiency in the calculation of the matrices. Finally, the equation for the modal analysis can be obtained as follows:

$$\mathbf{M}^*\delta\ddot{\mathbf{q}}_i + \mathbf{C}^*\delta\dot{\mathbf{q}}_i + \mathbf{K}^*\delta\mathbf{q}_i = 0. \tag{48}$$

3. Numerical results and discussion

Fig. 4 shows a planar beam structure (that consists of two beams) that rotates with constant angular speed Ω_s. In the figure, $\bar{X}^i - \bar{Y}^i$ denotes the ith local reference frame and β denotes the angle between the two beams. The geometric and the material properties of the beams are shown in Table 1. Symmetric beam cross-sections with no eccentricity are employed to avoid coupling between bending and torsional motions. Beam structures consisting of such a long slender dimension may often be found in a space robot structure which has several slender arms. Four local reference frames are employed for the proposed modeling method, which is explained in the previous section. Total 32 beam elements having equal length are employed for the finite element procedure. As the angular speed Ω_s varies (when the angle β is 90°), the dynamic equilibrium position of the free end point P is obtained by employing three methods: single reference frame method, multiple reference frame method, and a fully nonlinear finite element method (see Ref. [17]). The results obtained with the fully nonlinear finite element method are employed for the verification purpose. The horizontal and the vertical

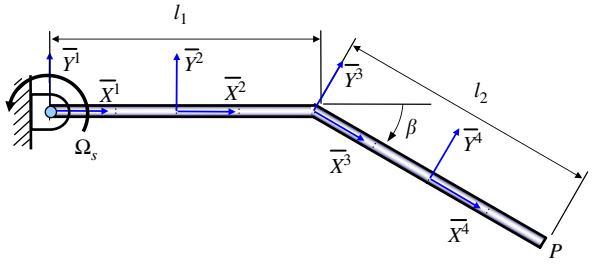

Fig. 4. Configuration of a rotating 2-beam structure.

Table 1
Properties of the 2-beam structure

Notation	Description	Numerical data
E	Young's modulus	7×10^{10} N/m^2
ρ	Mass per unit length	$1.2 \times$ kg/m
I	Area moment of inertia	2×10^{-7} m^4
A	Cross-section area	4×10^{-4} m^2
l_1	Length of beam 1	5 m
l_2	Length of beam 2	5 m

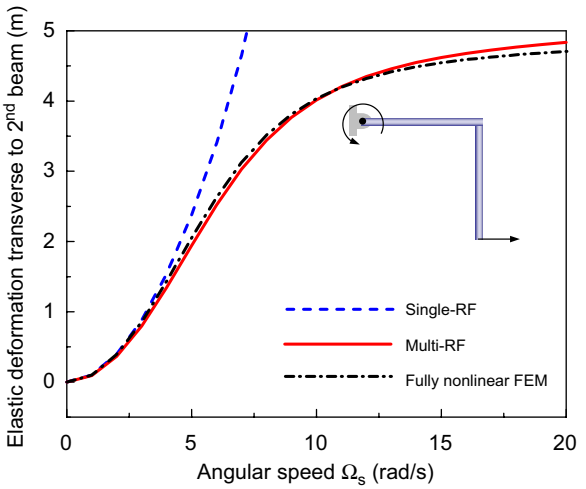

Fig. 5. Elastic deformation transverse to 2nd beam at the free end with the two methods ($\beta = 90°$).

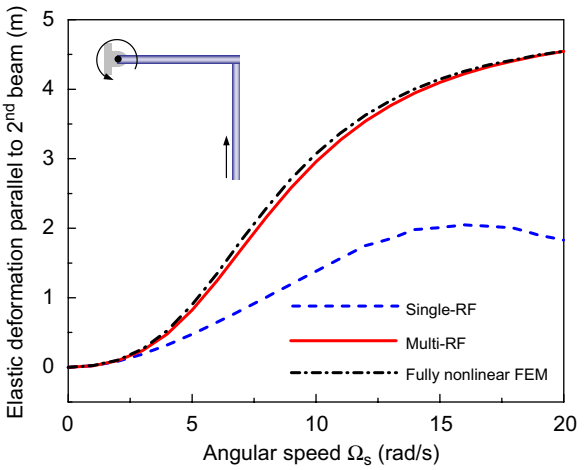

Fig. 6. Elastic deformation parallel to 2nd beam at the free end with the two methods ($\beta = 90°$).

elastic deformations, which are measured with respect to the first local reference frame $\bar{X}^1 - \bar{Y}^1$, are shown in Figs. 5 and 6, respectively. These figures indicate that the results obtained by employing multiple reference frames are in good agreement with those of the fully nonlinear finite element method. However, the accuracy

of the results obtained by employing a single reference frame deteriorates as the angular speed increases. The accuracy of the modal analysis depends on that of the dynamic equilibrium analysis since the equations for the modal analysis are obtained by linearizing the equations of motion at the dynamic equilibrium position. Therefore, it can be concluded from the above results that the accuracy of the modal analysis obtained with a single reference frame deteriorates as the angular speed of the structure increases.

Figs. 7–9 show the variations of the lowest three natural frequencies of the 2-beam structure versus the angular speed when β is 0°, 45°, and 90°, respectively. The two methods are employed to obtain the results: the single reference frame method and the multiple reference frame method. As shown in Fig. 7, the two results are in reasonable agreement when the angle β is 0°. The natural frequencies increase as angular speed increases. This phenomenon is well known as the stiffening effect of the rotating structure. However, as the angle β increases (as shown in Figs. 8 and 9), the disagreement between the two results increases. Especially, the disagreement becomes more significant with the second and the third natural frequencies. Since the natural frequency results of the single reference frame method are obtained by employing inaccurate dynamic equilibrium position, the accuracy of the modal analysis results deteriorates as the angle β and the angular speed increase.

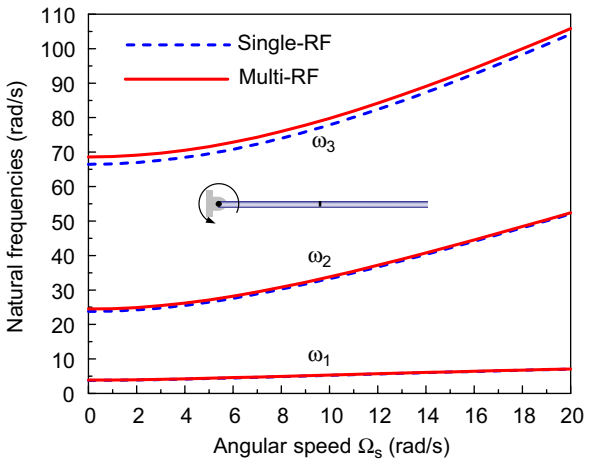

Fig. 7. The lowest three natural frequency variations versus angular speed obtained with the two methods ($\beta = 0^\circ$).

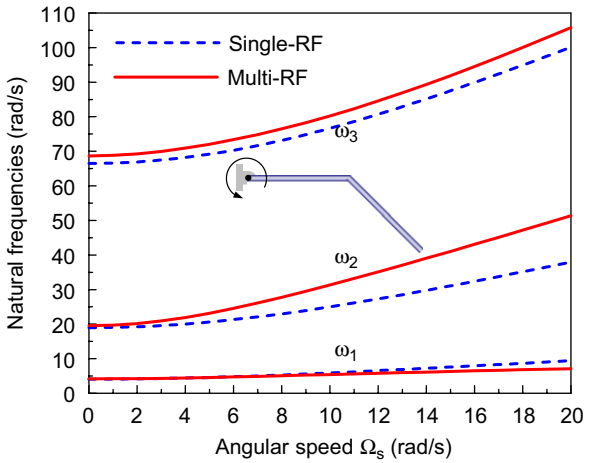

Fig. 8. The lowest three natural frequency variations versus angular speed obtained with the two methods ($\beta = 45^\circ$).

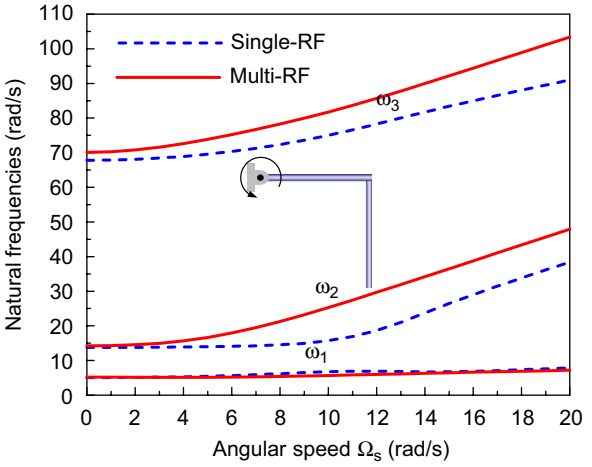

Fig. 9. The lowest three natural frequency variations versus angular speed obtained with the two methods ($\beta = 90^\circ$).

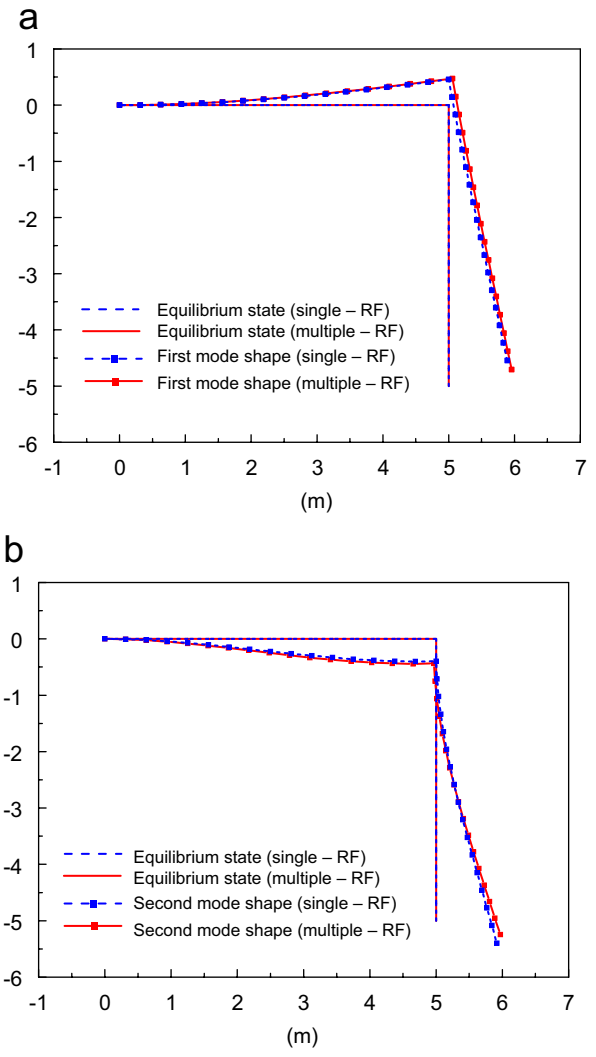

Fig. 10. Comparison of mode shapes obtained by single and multiple reference frame methods ($\Omega_s = 0$ rad/s, $\beta = 90^\circ$).

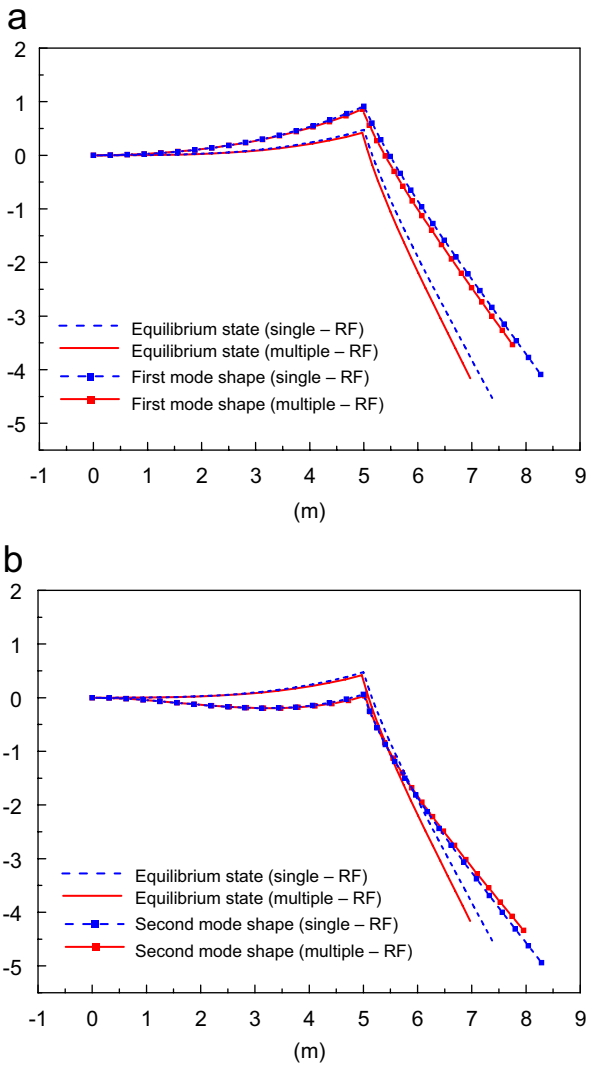

Fig. 11. Comparison of mode shapes obtained by single and multiple reference frame methods ($\Omega_s = 5\,\text{rad/s}$, $\beta = 90^\circ$).

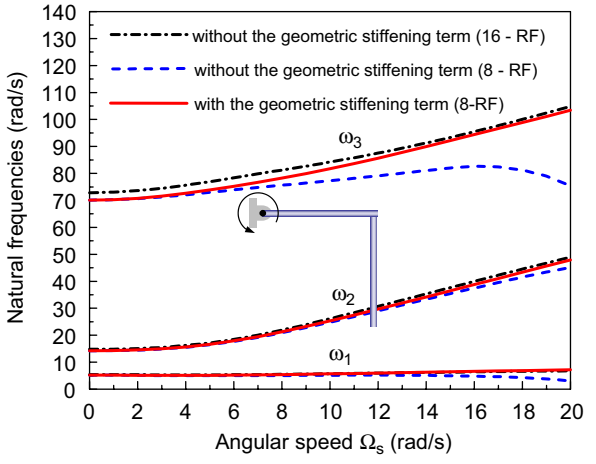

Fig. 12. The effect of the geometric stiffening term and multiple reference frames on the natural frequencies.

Table 2
Convergence of natural frequencies versus number of reference frames when the geometric stiffening term is absent or present

RF	Geometric stiffening term absent			Geometric stiffening term present		
	ω_1	ω_2	ω_3	ω_1	ω_2	ω_3
2	Fail to obtain			6.40	34.61	63.77
4				6.97	41.85	87.41
6				7.11	46.46	96.21
8	3.05	45.27	75.75	7.19	48.07	103.21
12	6.08	48.19	100.23	7.27	49.13	106.72
16	6.72	49.00	104.12	7.33	49.51	107.89

$\Omega_s = 20$ rad/s and $\beta = 90^\circ$. Units: rad/s.

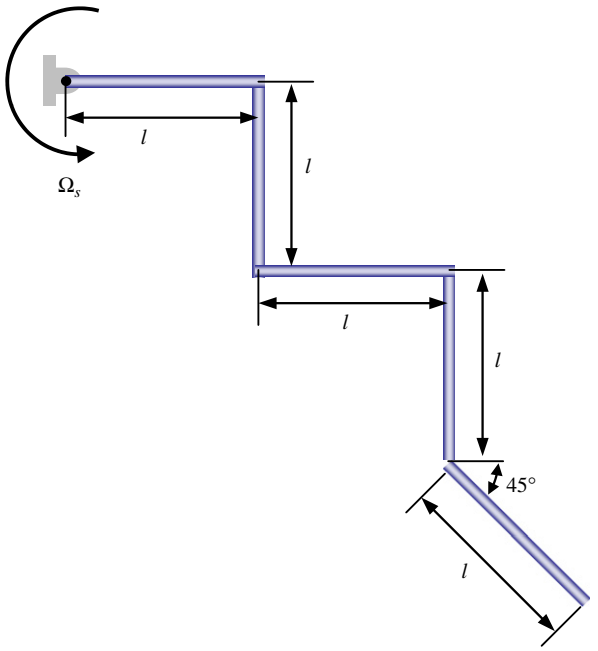

Fig. 13. Configuration of a rotating 5-beam structure.

Fig. 10 shows the first and the second mode shapes of the 2-beam structure when $\Omega_s = 0$ rad/s and β is 90°. The equilibrium positions are also given in the figure. The results obtained by the single reference frame method and the multiple reference frame method are relatively in good agreement. However, as shown in Fig. 11, the discrepancy between the two results obtained by the two methods increases as the angular speed increases. Fig. 11 also shows that the foreshortening effect cannot be considered with the single reference frame method while it can be well considered with the multiple reference frame method.

Fig. 12 shows the variations of the lowest three natural frequencies of the 2-beam structure (versus the angular speed) when β is 90°. Eight reference frames are employed to obtain the solid line results. The dotted line and the broken solid line results are obtained without the geometric stiffening term shown in Eq. (27). As shown in the figure, even if the geometric stiffening term is not included, converged solutions can be obtained with enough number of reference frames. However, if the geometric stiffening term is considered, faster convergence can be achieved with less number of reference frames. In general, including the geometric stiffening term is more efficient than increasing the number of reference frames to save computing time.

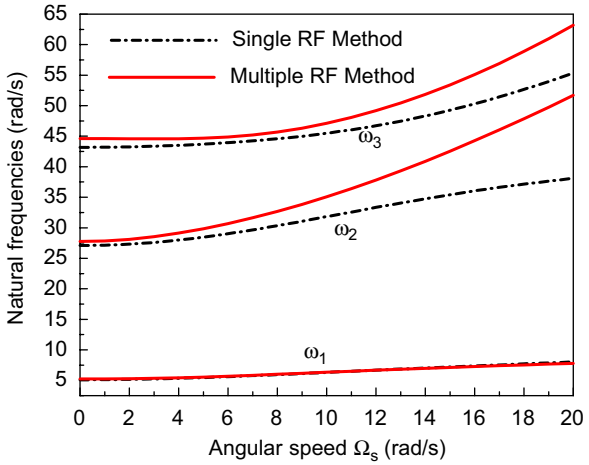

Fig. 14. The lowest three natural frequencies of 5 beam structure versus angular speed obtained with the multiple reference frame method and the single reference frame method.

To investigate the effect of the geometric stiffening on the convergence trend of the multireference frame method, the lowest three natural frequencies (versus the number of reference frames) are tabulated in Table 2. The 2-beam structure ($\beta = 90^\circ$) is employed and 48-beam elements are used to obtain the natural frequencies. As shown in the table, if the geometric stiffening term is absent, it is difficult to obtain accurate natural frequencies. The only way to achieve reasonable accuracy (when the geometric stiffening term is absent) is to increase the number of reference frames sufficiently. But that will cost much computing time.

As the last numerical example, a multibeam structure that consists of five beams is shown in Fig. 13. The geometric and the material properties of the five beams are same as those given in Table 1 except the length. Here, the length of a beam is 2 m. Total 15 reference frames and 60 beam elements are employed for the analysis in which the geometric stiffening term is considered. The results (the lowest three natural frequencies versus angular speed) obtained by employing the multiple reference frame method and the single reference frame method are compared in Fig. 14. As shown in the figure, the discrepancy between the two results is more significant in higher natural frequencies.

4. Conclusion

In this study, a modeling method employing multiple reference frames is proposed to find the modal characteristics of rotating structures that consist of multibeams. In the modeling method, a geometric stiffening term is included to accelerate the convergence of solutions. If the geometric stiffening term is not included, one should employ more reference frames to achieve the corresponding convergence. It is shown that the results obtained by employing the multiple reference frame method are more accurate than those obtained by employing the single reference frame method. This study shows that one should be very careful to employ a finite element code to perform modal analysis of rotating structures. Especially, when the angles among the beams of the multibeam structure increases, a finite element code employing a single reference frame could provide inaccurate results. Lastly, the formulation suggested in the present work can be applied to any three dimensional structures even if only planar motion examples are solved in the present study. Also, even if only beam element is employed in the present study, more general structural elements (like plates and shells) can be also incorporated into the formulation.

Acknowledgment

This work was supported by the research fund of Hanyang University (HY-2004-I).

References

[1] J. Ho, Direct path method for flexible multibody spacecraft dynamics, *Journal of Spacecraft and Rockets* 14 (1977) 102–110.

[2] A. Shabana, Dynamics of inertia variant flexible systems using experimentally identified parameters, *Journal of Mechanism, Transmissions, and Automation in Design* 108 (1986) 358–366.

[3] A. Shabana, R. Wehage, Variable degree of freedom component mode analysis of inertia variant flexible mechanical systems, *Journal of Mechanical Design* (1982) 1–8 No. 82-DET-93.

[4] T. Kane, R. Ryan, A. Banerjee, Dynamics of cantilever beam attached to a moving base, *Journal of Guidance, Control, and Dynamics* 10 (1987) 139–151.

[5] H. Yoo, R. Ryan, R. Scott, Dynamics of flexible beams undergoing overall motions, *Journal of Sound and Vibration* 181 (2) (1995) 261–278.

[6] S. Seo, H. Yoo, Dynamic analysis of flexible beam undergoing overall motion employing linear strain measures, *AIAA Journal* 40 (2) (2002) 319–326.

[7] D. Choi, J. Park, H. Yoo, Modal analysis of constrained multibody systems undergoing rotational motion, *Journal of Sound and Vibration* 280 (2005) 63–76.

[8] E. Christensen, S. Lee, Nonlinear finite element modeling of the dynamics of unrestrained flexible structures, *Computer and Structures* 23 (1986) 819–829.

[9] H. Yoo, S. Shin, Vibration analysis of rotating cantilever beams, *Journal of Sound and Vibration* 212 (1998) 807–828.

[10] D. Hodges, Review of composite rotor blade modeling, *AIAA Journal* 28 (1990) 561–565.

[11] M. Singh, A. Abdelnaser, Random response of symmetric cross-ply composite beams with arbitrary boundary conditions, *AIAA Journal* 30 (1992) 201–210.

[12] V. Yildirim, Out-of-plane bending and torsional resonance frequencies and mode shapes of symmetric cross-ply laminated beams including shear deformation and rotary inertia effects, *Communications in Numerical Methods in Engineering* 16 (2000) 67–74.

[13] S. Nagaraj, Refined structural dynamics model for composite rotor blades, *AIAA Journal* 39 (2001) 339–348.

[14] H. Yoo, J. Chung, Dynamics of rectangular plate undergoing prescribed overall motion, *Journal of Sound and Vibration* 239 (1) (2001) 123–137.

[15] A. Shabana, *Dynamics of Multibody Systems*, Cambridge University Press, Cambridge, 1998.

[16] P. Nikravesh, *Computer-Aided Analysis of Mechanical Systems*, Prentice-Hall., Inc., Englewood Cliffs, NJ, 1988.

[17] ANSYS User's Manual, *Structural Analysis Guide*, ANSYS Inc., 1998.